Core/shell cellulose-based microspheres for oral administration of Ketoprofen Lysinate

Vincenzo Guarino,[1] Tania Caputo,[1] Paola Calcagnile,[2] Rosaria Altobelli,[1] Christian Demitri,[3] Luigi Ambrosio[1]

[1]Department of Chemical Sciences & Materials Technology, Institute for Polymers, Composites and Biomaterials, National Research Council of Italy, 80125 Naples, Italy
[2]IMAST SCaRL, Piazza Bovio 22, 80133 Naples, Italy
[3]Department of Engineering for Innovation, University of Salento, Lecce, Italy

Abstract: Herein, we propose the fabrication of a new carrier with core/shell structure—inner core of cellulose acetate (CA) coated by a micrometric layer of chitosan (CS)—fabricated through an integrated process, which combines Electro Dynamic Atomization (EDA) and layer-by-layer (LbL) technique. We demonstrate that CA based microspheres possess a unique capability to relevantly retain the drugs—that is, Ketoprofen Lysinate (KL)—along the gastric tract, while providing a massive release along the intestine. CS shell slightly influences the morphology and water retention under different pH conditions, improving drug encapsulation without compromising drug release kinetics. *In vitro* studies in simulated gastric and intestine fluids (SGF, SIF) with physiological enzymes, show a moderate release of LSK during the first 2 h (ca. 20% at pH 2), followed by a sustained release during the next 6 h (ca. 80% at pH 7). The obtained results demonstrate that CA-based microspheres hold strong potential to be used as carriers for a delayed oral administration of anti-inflammatory drugs. © 2018 Wiley Periodicals, Inc. J Biomed Mater Res Part B: Appl Biomater 00B: 000–000, 2018.

Key Words: electrofluidodynamics, cellulose acetate, chitosan, ketoprofen lysinate, oral delivery

How to cite this article: Guarino V, Caputo T, Calcagnile P, Altobelli R, Demitri C, Ambrosio L 2018. Core/shell cellulose-based microspheres for oral administration of Ketoprofen Lysinate. J Biomed Mater Res Part B 2018:00B:000–000.

INTRODUCTION

Oral route is considered the most convenient and comfortable means of administering drugs to patients.[1] In the last few years, several methods have been used to improve oral bioavailability of drugs such as Ketoprofen, having poor water solubility and limited absorption mechanisms, according to the Biopharmaceutical classification system (BCS). Ketoprofen—also known as 2–(3-benzoyl phenyl) propionic acid—is an anti-inflammatory drug with analgesic and antipyretic effects, widely used to cure acute and chronic inflammatory diseases and in the treatment of rheumatoid arthritis. Some studies have demonstrated that its dissolution rate from solid dispersion can be influenced by several chemical and physical factors (i.e., local pH condition, concentration gradients), which drastically limit the bioavailability in oral treatments.[2] In particular, lysinate salt form—that is, Ketoprofen Lysinate (KL)—may offer similar anti-inflammatory effects in the symptomatic treatment of some chronic inflammatory diseases, with the additional advantage in terms of pharmacokinetics and tolerability with respect to ketoprofen. However, relevant shortcomings mainly concern their half-life—generally shorter than 2 h, as well as the uncontrolled degradation of molecules under the activity of digestive enzymes along the gastric tract, which drastically limit the therapeutic effect of active principles.[3]

In the last decade, many studies have been focused on the design of "drug delivery systems" through a fine control of the release rate for a site-specific delivery with reduced side effects and improved therapeutic efficacy and safety.[4] In particular, a growing interest is emerging for "chronotherapeutic" drug delivery systems[5] able to release a specific concentration of drug at specific times, for example, in correspondence to specific symptoms exacerbation (i.e., early morning pathologies).[6] To develop an efficient chronotherapy of such diseases, it is required that chrono-programmed carriers might be specifically designed to release active principle only when necessary, by preordered kinetic rates to selectively meet biological targets.[7]

Recently, extensive researches have been addressed to investigate the suitability of ionic polymers—that is, alginates, chitosans, haluronan, and cellulose derivates—to fabricate pH-sensitive micro and/or platforms with controlled mechanisms of drug release to be successfully used in

different applicative contexts—that is, tissue engineering,[8] drug delivery,[9] nanomedicine,[10] cancer models.[11] Among them, positive charged polysaccharides, such as chitosan, have been largely used as matrices or molecular excipients, thanks to some important features in terms of biocompatibility, non-toxic effects and selective degradation in biological fluids at different pH conditions.[12,13] In particular, CS has been investigated for the fabrication of innovative oral administration systems able to adhere to the mucosal surface thus mediating reversible epithelial tight junctions opening[14] along the intestine tract. Indeed, CS may also assist the protective function of the mucous lining along the digestive apparatus (i.e., oral cavity, esophagus). However, relevant constrains have been reported for CS in terms of drug administration control in the stomach, due to its rapid dissolution in the presence of strongly acid pH values (pH < 2.0). Hence, it is growing the fabrication of drug release systems chemically stable in the highly acidic environments, but able to rapidly dissolve in the presence of neutral (or slightly basic) environmental conditions.[15] For instance, CA has been recently used to design nanoscale drug depots in the form of core-shell fibers able to release ferulic acid (FA).[16] Likewise, ethylcellulose (EC) has been used to successfully encapsulate poorly water-soluble anticancer drugs such as tamoxifen, so as to control the carrier dissolution into the stomach, thus promoting the drug release to the proximal segment of the small intestine.[17] However, the efficacy with ketoprofen based molecules has not been completely demonstrated, mostly because of their chemical instability and relevant side effects—in turn, ascribable to the presence of aggressive solvents or to the use of additive chemical procedures, such as crosslinking and grafting, which are often required to stabilize bioactive molecules into the carrier[18]).

In this context, the addition of ionic polymer layers able to be selectively dissolved under different environmental stimuli—such as CS—may be suitable to improve polar interactions among drug molecules in the diffusing media, thus influencing carrier properties (i.e., hydrophilicity, crystallinity) for a more accurate control drug encapsulation, and prolonged molecular release.[19–21] In this work, new cellulose based carriers have been engineered via electrofluidodynamics (EFDTs) to achieve a sustained release of KL for several hours after the in vitro administration. EFDTs include a set of innovative top down technologies based on simple fabrication processes able to design innovative devices with restrained manufacturing costs but high functional complexity, with great benefits in terms of pharmaceutical applications.[22] Among them, electrospraying, as a counterpart of electrospinning, is currently considered the gold standard process to prepare microspheres for drug delivery applications.[23] Although different devices for controlled drug delivery have been successfully fabricated via coaxial configuration,[24] the implementation of new setups based on the application of electrical forces to single-fluid blending still represents a big challenge to minimize the electrofluidodynamic process complexity.[25] Currently, new possibilities for the fabrication of advanced functional materials are emerging by the combination of electrofluidodynamics with other consolidated technologies (i.e., emulsion, self-assembly).[26,27]

Herein, core shell devices for KL release have been fabricated by a two-step process combining electrofluidodynamics and layer by layer techniques. In particular, CA microparticles have been fabricated via electrohydrodynamic atomization.[28] A core shell structure was imparted by a controlled deposition of CS macromolecules onto CA surface through a layer by layer strategy. In this case, the cellulose acetate acts as gastro-resistant system, thus limiting the drug release into the stomach and providing a delayed release of drugs along the first tract of intestine. Meanwhile, chitosan shell prevents any uncontrolled release of drug along the first tract of digestive apparatus (i.e., oral cavity, esophagus), also supporting the local residence of CA microspheres to the contact with stomach mucosa. Herein, we have investigated the morphological properties and water retention of CA based carriers to elucidate about their mechanisms of gastro-resistance and delayed in vitro release of KL. For this purpose, particle morphology was examined by scanning electron microscopy (SEM) imaging. The water adsorption was also investigated in bi-distilled water and in different physiological fluids under different pH conditions.

MATERIALS AND METHODS
Materials
Cellulose acetate powder (Mn 30 kDa, 39.8 wt % acetyl), low molecular weight chitosan powder (deacetylation degree DD = 75–85%), sodium hydroxide (NaOH), potassium dihydrogen phosphate (KH_2PO_4), sodium chloride (NaCl), amylase powder, pancrease powder, lysozyme from chicken egg white, Kaiser test kit, acetic acid ($C_2H_4O_2$), acetone (C_3H_6O), hydrochloric acid (HCl) 37%, were all supplied by Sigma-Aldrich. KL was kindly supplied by Dompè. Simulated gastric fluid (SGF) was prepared by dissolving 2.0 g of sodium chloride, 3.2 g of pepsin and 7.0 mL of concentrated (37%) HCl in distilled water to obtain a solution having a total volume of 1 L (USP Test Solution Method). Simulated intestinal fluid (SIF) was prepared by adding 190 mL of 0.2 N NaOH, 400 mL of distilled water and 10 g of pancreatin to an aqueous potassium hydrogen phosphate solution, then adjusting the pH of the resulting solution to 7.5, also adding distilled water to obtain a solution having a total volume of 1 L (USP Test Solution Method)

Core-shell system fabrication
Fabrication of CA microspheres via electrofluidodynamics. CA solution was prepared by dissolving 0.05 g/mL, into a 80:20 (volume ratio) mixture of acetone and bidistilled water. The final solution was obtained by adding KL under magnetic stirring at room temperature until a clear solution was obtained. Atomized particles were obtained using a commercially available electrospinning setup (NF-500, MECC, Japan) equipped with a tailor-made collector to collect stable polymer droplets under controlled magnetic stirring as described in Figure 1—left side. The polymer solution was placed in a 5 mL
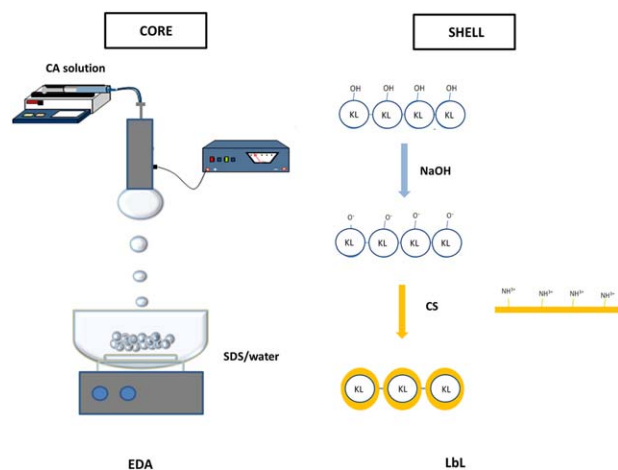
FIGURE 1. Scheme of two step preparation of CA/CS systems: fabrication of CA microspheres via electro dynamic atomization and LbL deposition of the CS shell onto the CA surface.

plastic syringe by connecting power supply to a 22 Gauge needle. Once the pump system was working, particles were collected into a aqueous coagulation bath containing sodium dodecyl sulfate (SDS), at a concentration of 5 mM—placed under magnetic stirring during the process. Different process parameters were selected to optimize the final particle morphology: in particular, optimal microparticles were fabricated by setting a distance of 15 cm, a voltage of 18 kV and a flow rate of 2.5 mL/h. The process was carried out in a vertical configuration at 23°C and 50% relative humidity. These conditions allowed obtaining wall materials with different average diameter, as estimated by image analysis techniques (image J, ver 1.37).

Preparation of CS shell via layer by layer technique. Microparticles were preliminary soaked in an alkaline solution containing NaOH (0.05 M) for 10 s to activate CA surfaces (Figure 1—right side). Then, they were immersed into a CS solution, 0.02 mg/mL into 99:1 (volume ratio) mixture of bi-distilled water and acetic acid, to trigger the chitosan crosslinking. Hence, the resulting system was kept under orbital continuous stirring at 25°C for 12 h for the coating stabilization and particle disaggregation. Finally, the microspheres were filtered, washed twice with PBS and dried at 37°C for the storage.

Chemical analyses

Chitosan coating was preliminarily investigated using Kaiser test kit (50 mL of solution containing 80% v/v phenol/ethanol, % KCN in H_2O/pyridine, 6%w/v Ninhydrin in ethanol—Sigma Aldrich, Italy) which is a qualitative method to reveal the presence of free primary amino groups on the surface of the system. The reaction of ninhydrin with primary amines is recognized by the presence of a characteristic intense blue staining. To this purpose, certain amount of microspheres (ca. 5 mg) was placed in a small test tube and drop-to-drop dipped with he previous solution. Successively, tubes were placed in hot water and the reaction left to go

on for 5 min. The presence of Chitosan was also detected through FTIR analysis. FTIR spectra were recorded using a Fourier Transform Infrared Spectrophotometer (FT-IR Frontier Dual Range Perkin Elmer), operating from 4,000 to 500 cm^{-1}, at resolution of 4 cm^{-1}. FTIR spectra were obtained from KBr pellets. Moreover, spectra of CA specimens were also taken as negative control.

Morphological analyses

The morphology of the CS-CA and CA systems was investigated both *via* optical (Dino-Lite Digital Microscope, Dino-Lite Europe, The Netherlands) and SEM, (Zeiss-EVO40, Carl Zeiss Group, Germany). By means of optical microscopy, the dimensional analysis of the produced microspheres was performed. Images at different magnifications were acquired and, among them, 20×-magnified ones were selected for the next analysis. Dimensional analysis of both CS-CA and CA systems was carried out, to perform a dimensional comparison and evaluating the difference in size due to the presence of chitosan coating onto their surface. The average diameter was estimated (using the DinoCapture 2.0 software), as the average calculated over one-hundred specimens for each group. Subsequently, SEM images were recorded in high-resolution mode with 20 kV of applied voltage. The SEM analysis was carried out mainly to investigate the inner section and the shape of the CA and CA-CS systems to detect main morphological differences between the two groups.

Water absorption

Water retention properties of both kinds of systems were analyzed and compared. A certain amount of microspheres (about 15 mg for each typology) was immersed into deionized water for 15 min and then filtered. The excess of water was gently removed through absorbing article. After one hour, the weight was measured and the mass variation was calculated according to the following equation:

$$\text{Mass variation} \% = \frac{M_f - M_i}{M_i} \cdot 100 \qquad (1)$$

where M_f was the mass of the samples after dipping in water bath and M_i the dry mass of the same type. Then, the dynamic mass variation was investigated,[29–31] so as to measure the water absorption due to the external chitosan coating. To this aim, the weight of the samples extracted from the water bath after 1 h, was recorded continuously.

The swelling behavior of CA-CS and CA in Simulated Gastric Fluids (SGF) and Simulated Intestinal Fluid (SIF), over 8 h, was then investigated. Specifically, a certain amount of microspheres—about 10 mg—was immersed into a SGF bath, kept at a temperature of 37°C for 2 h, and successively dipped into a SIF bath, under the same conditions, for subsequent 6 h. The mass variation was monitored every 30 min during the firsts two hours and every hour for the remaining experimental time. The percentage mass variation was calculated as reported in Eq. (1), where M_f is the mass of the samples after dipping in SIG/SIF bath and

M_i is the dry mass of the same sample type. All tests were conducted in triplicate for both sample populations.

In vitro release

In vitro KL release tests were conducted in sink condition simulating the biological fluids. KL loaded systems were placed into 1 mL of release medium and incubated at 37°C under shaking. SGF and SIF media, prepared according to the European Pharmacopoeia, were selected as releasing media. In particular, tests were also performed in the presence of physiological concentration of intestinal enzymes as follows: 93.8 U/mg amylase and 65.4 U/mg pancreases in SIF. Moreover, lysozyme (30 µg/mL in SIF) was added to evaluate the effect on chitosan shell degradation at physiological concentration. Released KL amount was evaluated at 260 nm using a UV-Vis spectrophotometer (Perkin-Elmer Victor X3). A quantity of 500 µL of the solution was replaced by fresh medium at each time step for measurements. All tests were conducted in triplicate for both sample populations, using CA samples as controls. The encapsulation efficiency and drug loading were calculated as reported in Refs. 32 and [33], using the following relations:

$$EE \text{ (Encapsulation Efficiency)} = (m - m_f)/m$$

where m is the total KL amount and m_f is the free amount of KL.

$$LC \text{ (Loading Capacity)} = m - m_f/m_c$$

where m_c is the total amount of KL.

Statistical analysis

The experimental data are presented as mean ± SD. The results from the *in vitro* dissolution tests were analyzed using the t-student test with a threshold significance level of 0.05.

RESULTS

In this work the study of CA microspheres coated by CS layer has been reported. Kaiser tests have been variously assessed to prove the stability and qualitatively validating the protective function of CS coating (Figure 2). At the first attempt, it was observed that in the case of KL unloaded systems, the presence of CS coating conferred a vivid and uniform purple staining to the carrier, related to a slight solubilization of the thin CS layer in the solution. Conversely, a lack of coloration was easily noticed in the case of plain CA systems, probably due to the rapid and complete dissolution of the polymer matrix just after few minutes of dipping. The presence of a CS coating was also confirmed by IR analyses performed on both coated and uncoated systems. The IR spectra recorded in the case of CS/CA and CA microspheres have been shown in Figure 3. In the spectrum of CS/CA, a broad band centered at about 3,232 cm^{-1}, corresponding to the vibration stretching related to the overlapping of the O–H and N–H bonds, was recognized. In the case of CA, peaks at 2,973, 2,933, 2,881, 1,413, 1,310, and 1,230 cm^{-1} were
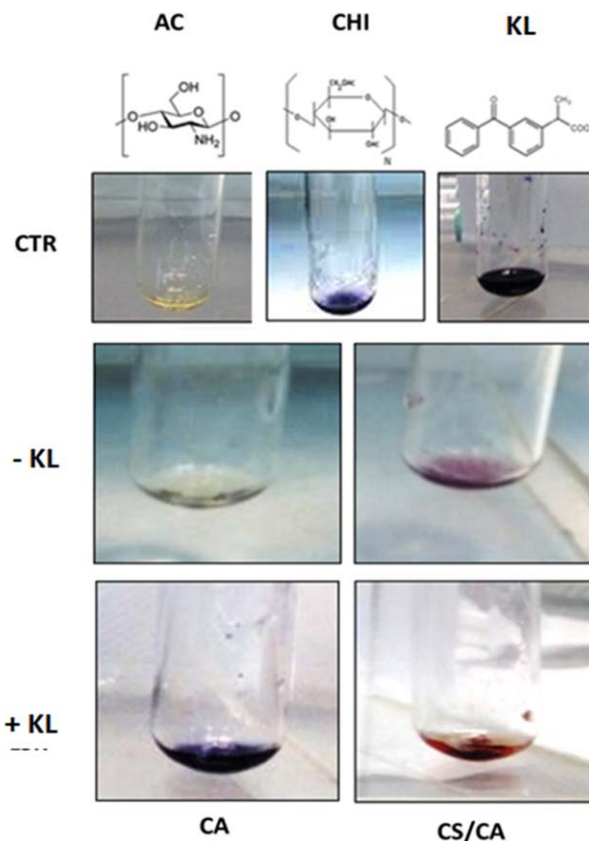

FIGURE 2. Chemical analyses to detect the presence of CS shell: Kaiser staining test of CA and CS/CA microspheres with and without KL.

observed, due to the symmetric or asymmetric CH$_2$ stretching vibrations of pyranose ring. Noteworthy, the characteristic absorption bands of CS were also identified at 1,649 and 1,558 cm^{-1}, corresponding to C–O stretching (amide I) and N–H bending (amide II), respectively. Additionally, several characteristic peaks of KL were also recognized. However, most of them were partially covered by the main peaks associated to polymer matrices and/or coating, therefore, it is quite difficult to analyze differences in the KL amount among samples.

A slightly elliptical shape of CA and CS/CA microspheres— < 10%—was revealed by optical images; this effect was mainly due to the droplet elongation occurring into the coagulation bath, prior to the droplet stabilization (Figure 4—in the square). Morphological characterization was also supported by a quantitative analysis via image analysis on selected images to evaluate the specific size distribution in the case of CA and CS-CA particles. No significant differences in the average diameter were detected under the simplified assumption of spherical shape approximation. More in detail, the mean diameter of the CS/CA microspheres was equal to 1.04 ± 0.22 mm; whereas the mean diameter of CA microspheres, used as a reference in this study, equal to 0.84 ± 0.14 mm. Further investigation performed on microsphere cross-section by SEM also indicated the presence of inner cavities in the body, probably acting as depots able to potentially host drugs or molecular
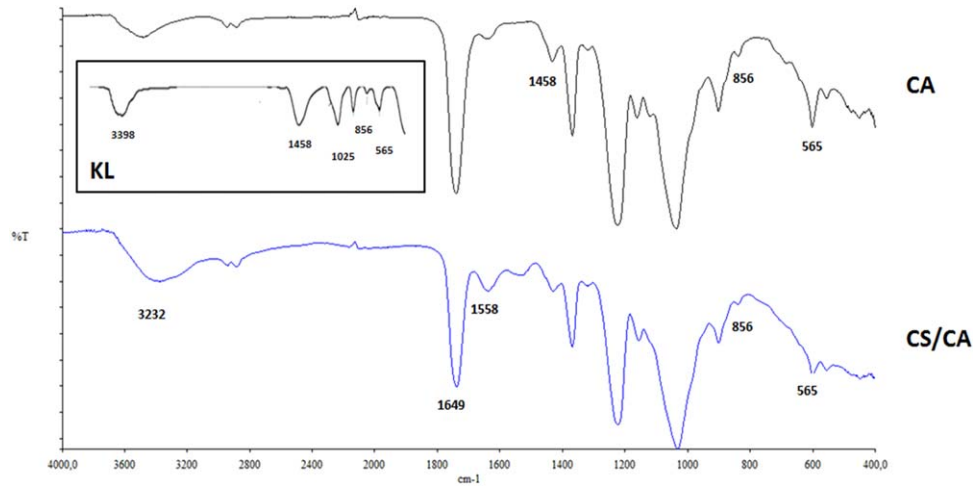
FIGURE 3. Comparison of FTIR spectra for CA (black) and CS/CA microspheres (blue), in the square, KL spectra.

species (Figure 4). Hence, the effect on the peculiar structure organization on selected chemical/physical properties such as water absorption capability, was further explored. Mass variation measurements have been performed in the case of CA and CS/CA (Figure 5). According to Eq. (1), a mass increase of $338.77\% \pm 31.26\%$ was estimated in the case of CS/CA. No considerable differences were detected with respect to nude CA, showing a mass increase of
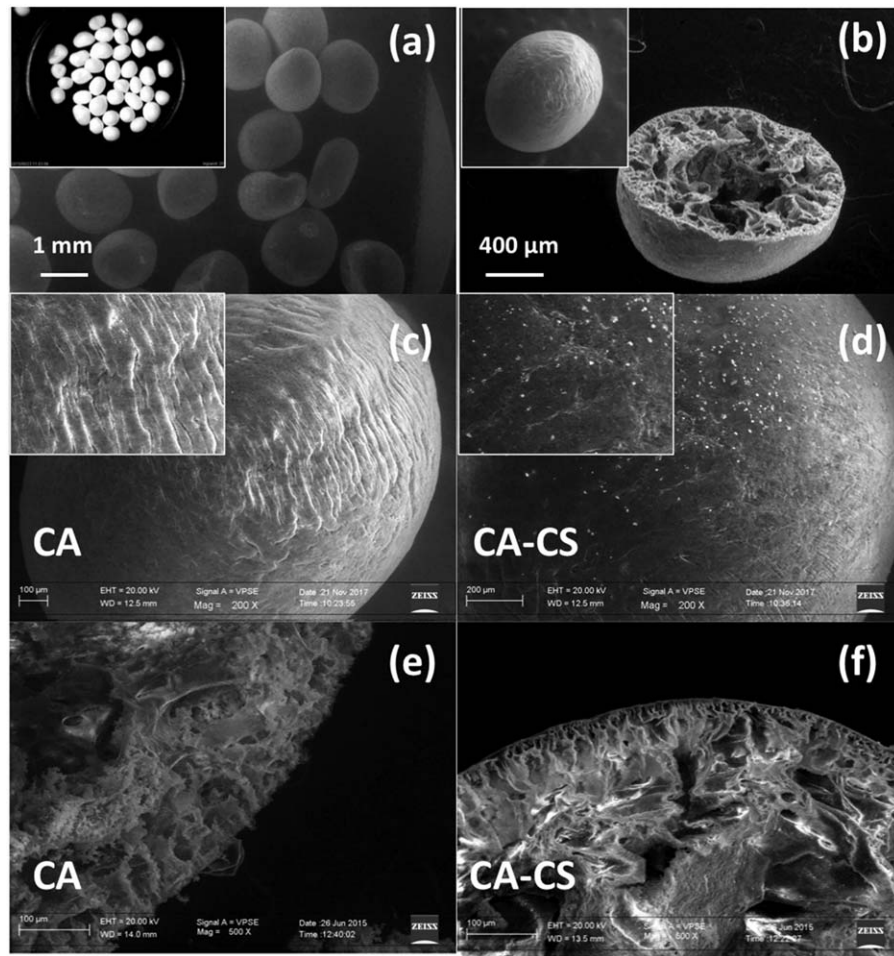

FIGURE 4. SEM images of (a) surfaces (optical image in the square) and (b) cross-section of CA; (c) detail of the surface of CA and (d) CA-CS; (e) detail of the cross-section of CA and f) CS/CA.
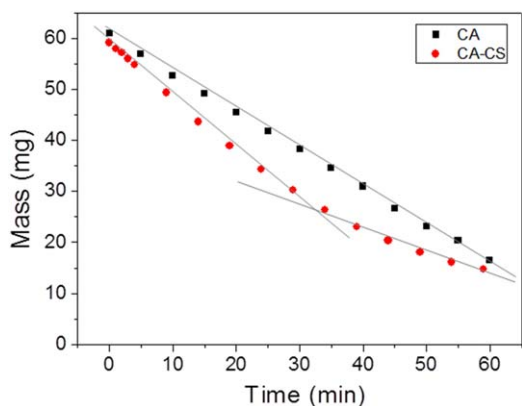
FIGURE 5. Mass versus time of CA (squares) and CA-CS (circles) microspheres, after being dipped in water for 15 min. All tests were conducted in triplicate for each time for both sample populations.

353.45% ± 5.92%. Conversely, different water retention were underlined by dynamic mass variation over time. Two curves representative of the reduction over time of the mass in the case of CA and CA/CS during water dipping have been reported inn Figure 5. Although the two curves reached a plateau for similar values, a significant difference was observed in terms of dynamic trends during the first two hours: in the case of CA microspheres, the data are well-fitted by one line only, −0.70 as slope, thus confirming their ability to absorb water macromolecules at the surface. In this case, the mechanism is basically regulated by a mere adsorption of water molecules onto the surface, due to the moderate hydrophilic behavior of CA. As for CA-CS microspheres, data are well-fitted by two different linear profiles, with 1.02 and −0.46 as slope, respectively. The effect of CS coating on mass variation dynamics was also confirmed by the mass variation curves in simulated physiological fluids (Figure 6), SGF and SIF, respectively, for CA and CS-CA systems. The higher increase, recorded in the case of CS/CA, is mainly ascribable to the hydrophilic properties CS coating during the first 2 h in the acid microenvironment (SGF
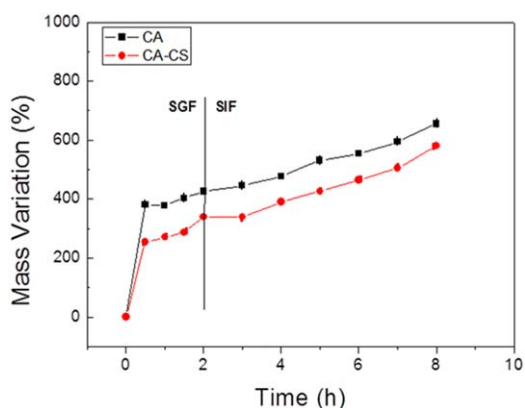

FIGURE 6. % Mass variation versus time: effect of chitosan coating onto the swelling mechanism of core shell systems under simulated environmental conditions of the digestive system: first 2 h in SGF and subsequent 6 h in SIF. All tests were conducted in triplicate for each time for both sample populations.
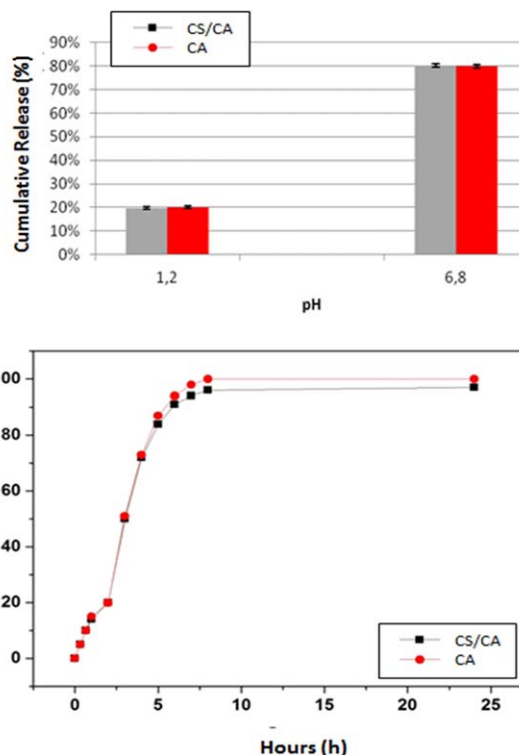

FIGURE 7. Total amount (%) and Cumulative release profiles (%) of KL loaded CA and CS-CS systems. All samples were conditioned into SGF (pH 1.2) for first 2 h, and SIF (pH 6.8) for next 6 h until the end of release. All tests were conducted in triplicate for each time for both sample populations.

solution). Then, CS layers progressively dissolves, thus exposing the surrounding CA core which drastically reduces their attitude to the water adsorption. This was confirmed by trends of mass variation recorder either in the case of CA then CS/CA conditioned in SIF solutions, solely ascribable to the adsorption mechanisms of CA matrix along next 6 h.

Lastly, *in vitro* KL release from CS/CA and CA microspheres was also investigated to validate their use for oral administration. Unremarkable differences between *in vitro* KL release profiles were detected in the presence of CS coating (Figures 7 and 8). In particular, basic studies performed in SGF showed only a reduced release of KL—about of 20%—independently on the presence of CS layer (Figure 7), while the most part of KL was released in SIF, during subsequent 6 hours. Further *in vitro* release studies in SIF enriched with selected enzymes such as amylase/pancrease at physiological concentration (pH 6.8) also showed release profiles (Figure 8) with similar trends, allowing for a release of only 10% of drug after 2 h until a complete release (i.e., 100% of KL) after 6 h [Figure 8(a)]. Similar behavior was also observed in SIF medium enriched with lysozyme at physiological concentrations [Figure 8(b)].

DISCUSSION

In this work, the investigation of new core-shell microcarriers fabricated by a two steps process based on the
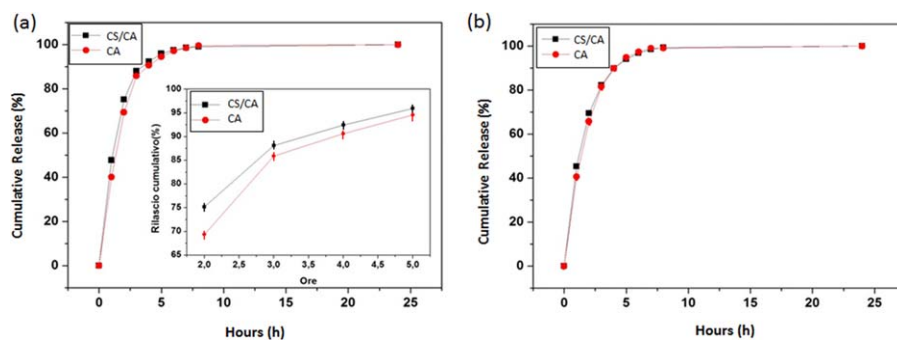
FIGURE 8. Cumulative release profiles (%) of KL loaded CA and CA-CS microspheres in SIF in the presence of (a) amylase/lipase or (b) Lysozyme at physiological concentration. All tests were conducted in triplicate for each time for both sample populations.

combination of electrofluidodynamic atomization and layer by layer deposition is proposed. The inner core made of CA is developed by an emerging technology recently patented by Guarino et al.[34] based on the fluid dynamic breaking of polymer solutions into macro-sized droplets and their subsequent precipitation into a chemically functionalized dipping bath. Moreover, a layer by layer strategy has been optimized to cover the microsphere by a chitosan shell as efficient coating to improve drug encapsulation without compromising molecular release. The chemical characterization based on the use of Kaiser tests and FTIR analyses confirmed the formation of an homogeneous thin chitosan layer onto the microsphere surface, by controlling the soaking procedure in NaOH solution. From morphological point of view, the presence of CS coating seems to not compromise the spherical-like shape of microcarriers, but slightly increases the average diameter of the final device—not over the 20% respect to the diameter of CA microspheres. Interestingly, a change in the structural organization is observed in the presence of CS layer. Nude CA systems show a characteristic structural organization of the surfaces, due to the presence of a highly porous wall surrounding an external skin. This is related to the occurrence of local solvent exchange mechanisms at the CA surface during the droplet dipping, at the preliminary stage, thus promoting the local formation of surface micro/macroscopic defects [Figure 4(c)]. Vice versa, CS/CA systems exhibit a more compact surface, probably due to effect of layer by layer deposition of CS which concurs to fill surface microcavities, also improving core shell interface [Figure 4(d)]. We have demonstrated that this peculiar structure organization concurs to particularize the chemical/physical properties in terms of water absorption capability. Mass variation measurements allowed clearly identifying two distinct water absorption mechanisms: the first is related to a more rapid absorption of water molecules by the presence of the highly hydrophilic CS coating while the second phenomenon is related to a slower mechanism of water molecules absorption into the cellulose acetate microcavities. In the presence of CS layer, this secondary water absorption mechanism is slower than those occurring in the case of nude CA, due to the covering effect of CS shell of surface microcavities, with potential

effects on molecular transport and delivery, as also confirmed by simulated tests in SGF and SIF media (Figure 5). These considerations have been also corroborated by *in vitro r*elease studies, performed to validate the effective use of microspheres for oral administration. We verified a drastic increase of encapsulated KL in the case of CS/CA—about 50% higher than those of CA ones—without recording any relevant drug loss during the coating procedure. This result may be explained by the effect of CS shell on the morphology at the interface with the surrounding CA core. Indeed, the reduction of local defects improves the interface stability, thus limiting the formation of preferential exit routes to drug molecules during water adsorption. Contrariwise, no differences between *in vitro* KL release profiles, respectively, 20% in SGF and 80% in SIF media—may be directly ascribable to the presence of CS coating, instead, mainly related to the local pH effect on the solubility of KL molecules. Indeed, KL acts as a weak acid and its solubility tends to rapidly increase for higher pH values until to be completely ionized at intestinal pH—from 5.8 to 6.5—so that it might be completely released along the upper small intestine tract.[31]

Other studies performed in SIF enriched with selected enzymes (i.e., amylase, pancrease) at physiological concentration (pH 6.8) to mimic native gastro-intestinal microenvironment further corroborate the idea that CS shell does not interfere with the mechanism of KL release. This is confirmed also in the case of lysozyme, an elective enzyme naturally present in biological fluids of the intestine deputed to promote the lysis of the bacterial cells, being able to cleave the glycosidic linkage between units of N-acetyl glucosamine and N-acetylmuramic acid.[35] We demonstrate that this result is not in contrast with the intrinsic attitude of this enzyme to dissolve chitosan macromolecules.[36] Indeed, the ability of lysozyme to trigger chitosan shell degradation is clearly manifested only over 10 days, not influencing the massive release of drug occurring by 6 h after the oral administration.

CONCLUSIONS
One of the main challenges in oral delivery currently concerns the improvement of drugs or molecular administration by the support of tailored systems able to deliver the

right dose of therapeutic agents along the intestine, preserving the gastric stroke. For this purpose, drug-loaded carriers have to protect the active principle from the harsh environment of the stomach, thus delivering it where the action mechanism, that is,—drug absorption—is required. In this context, it was demonstrated that muco-adhesive polymers—that is, CA and CS may be successfully used to assembly core-shell carriers able to locally guide drug administration. Indeed, their ability to change water absorption and swelling behavior in response to the environmental factors—such as ionic strength, temperature or pH—allows controlling chemical functionalities of the carrier—that is, hydrophilic, partially hydrophilic or hydrophobic groups such as hydroxyl, carboxyl, amide, and sulfate—able to promote a greater attachment and/or retention of dosage forms. CA based carriers with a peculiar core/shell organization—imparted by the combination of EFDTs and LbL, may be efficaciously used to directly interact with stomach and small intestine mucosae along the gastrointestinal tract, thanks to strong adhesive interactions exerted by muco-adhesive polymers (i.e., Van der Waal and hydrophobic interactions). Moreover, they are able to protect KL in acid microenvironment of stomach, providing a massive release—over 80%—along the intestinal tract. This is mainly ascribable to the capability of CA to retain the drug along the first tract, not dissolving at gastric pH. Moreover, the presence of additive CS layer concur improving KL encapsulation, due to the hydrophilic behavior and peculiar structure at the interface with surrounding CA substrate. Under different environmental conditions in the presence of specific enzymes, both microcarriers have shown a substantial delay in the release time (up to 3 h) followed by a sustained release of about 6 h of the drug, thus suggesting their use as a promising system for certain oral delivery applications in which a selective delivery of therapeutic agents along the intestine is required.

REFERENCES

1. Goldberg M, Gomez-Orellana I. Challenges for the oral delivery of macromolecules. Nat Rev Drug Discov 2003;2:289–295
2. Chuong MC, Palugan L, Su TM, Busano C, Lee R, Di Pretoro G, Shah A. Formulation of controlled-release capsules of biopharmaceutical classification system i drugs using niacin as a model. AAPS PharmSciTech 2010;11(4):1650–1661
3. Owens DR, Zinman B, Bolli G. Alternative routes of insulin delivery. Diabet Med 2003;20:886–898.
4. Sithole MN, Choonara YE, du Toit LC, Kumar P, Pillay V. A review of semi-synthetic biopolymer complexes: modified polysaccharide nano-carriers for enhancement of oral drug bioavailability. Pharmaceut Dev Technol 2017;22:283–295.
5. Mandal AS, Biswas N, Karim KM, Guha A, Chatterjee S, Behera M, Kuotsu K. Drug delivery system based on chronobiology—A review. J Controlled Release 2010;147:314–325.
6. Nainwal N. Chronotherapeutics—A chronopharmaceutical approach to drug delivery in the treatment of asthma. J Controlled Release 2012;163:353–360.
7. Ohdo S. Chronotherapeutic strategy: Rhythm monitoring, manipulation and disruption. Adv Drug Deliv Rev 2010;62:859–875.
8. Manferdini C, Guarino V, Zini N, Raucci MG, Ferrari A, Grassi F, Gabusi E, Squarzoni S, Facchini A, Ambrosio L, Lisignoli G. Mineralization occurs faster on a new biomimetic hyaluronic acid-based scaffold –Biomaterials 19 feb, 2010. Biomaterials 2010;31: 3986–3996.
9. Wang Q, Yu D-G, Zhang L-L, Liu X-K, Deng Y-C, Zhao M. Electrospun hypromellose-based hydrophilic composites for rapid dissolution of poorly water-soluble drug. Carbohydr Polym 2017;174: 617–625.
10. Peniche H, Peniche C. Chitosan nanoparticles: a contribution to nanomedicine. Polym Int 2011;60:883–889.
11. Guarino V, Cirillo V, Altobelli R, Ambrosio L. Polymer based platforms by electric field assisted techniques for tissue engineering and cancer therapy. Expert Rev Med Devices. 2015;12(1):113–129.
12. Guarino V, Caputo T, Altobelli R, Ambrosio L. Degradation properties and metabolic activity of alginate and chitosan polyelectrolytes for drug delivery and tissue engineering applications. AIMS Mater Sci 2015;2:497–501.
13. De la Fuente M, Raviña M, Paolicelli P, Sanchez A, Seijo B, Alonso MJ. (2010). Chitosan-based nanostructures: a delivery platform for ocular therapeutics. Adv Drug Deliv Rev 2010;62:100–117
14. Smith J, Wood E, Dornish M. Effect of chitosan on epithelial cell tight junctions. Pharmaceut Res 2004;21:43–49.
15. Sung HW, Sonaje K, Liao ZX, Hsu LW, Chuang EY. pH-responsive nanoparticles shelled with chitosan for oral delivery of insulin: From mechanism to therapeutic applications. Acc Chem Res 2012;45:619–629.
16. Yang G-Z, Li J-J, Yu D-G, He M-F, Yang J-H, Williams GR. Nano-sized sustained-release drug depots fabricated using modified triaxial electrospinning. Acta Biomaterialia 2017;53:233–241.
17. Li X-Y, Zheng Z-B, Yu D-G, Liu X-K, Qu Y-L, Li H-L. Electrosprayed spherical ethylcellulose nanoparticles for an improved sustained-release profile of anticancer drug. Cellulose 2017;24:5551–5564.
18. Nasser S, Sameen LH, Ghareeb MM. Preparation and evaluation of oral disintegrating tablets of ketoprofen by direct compression. Iraqi J Pharm Sci 2012;21:63–68.
19. Cerciello A, Auriemma G, Del Gaudio P, Cantarini M, Aquino RP. Natural polysaccharides platforms for oral controlled release of ketoprofen lysine salt. Drug Dev Ind Pharm 2016;42(12):2063–2069.
20. Kini AG, Dixit M, Kulkarni PK. Enhancement of solubility and dissolution rate of poorly water soluble drug by spray drying using different grade of chitosan. Int J Pharm Sci 2011;3;(Suppl. 2):231–235.
21. Guarino V, Cruz-Maya I, Altobelli R, Abdul Khodir WK, Ambrosio L, Alvarez Pèrez MA, Almaguer Flores A. Electrospun polycaprolactone nanofibres decorated by drug loaded chitosan nanoreservoirs for antibacterial treatments. Nanotechnology 2017;28: 505103.
22. Guarino V, Ambrosio L. Electrofluidodynamics: Exploring new toolbox to design biomaterials for tissue regeneration and degeneration. Nanomedicine 2016;11(12):1515–1518.
23. Guarino V, Wan Abdul Khodir WK, Ambrosio L. Biodegradable micro and nanoparticles by electrospraying techniques. (IF 1.5). J Appl Biomater Funct Mater 2012;10(3):191–196.
24. Liu Z-P, Zhang Y-Y, Yu D-G, Wu D, Li H-L. Fabrication of sustained-release zein nanoparticles via modified coaxial electrospraying. Chem Eng J 2018;334:807–816.
25. Yang Y-Y, Zhang M, Liu Z-P, Wang K, Yu D-W. Meletin sustained-release gliadin nanoparticles prepared viasolvent surface modification on blending electrospraying. Appl Surf Sci 2018;434:1040–1047.
26. Guarino V, Altobelli R, Cirillo V, Cummaro A, Ambrosio L. Additive electrospraying: a new route to process electrospun scaffolds for controlled molecular release. Polym Adv Technol 2015;26: 1359–1369.
27. Song Y, Chan Y-K, Ma Q, Liu Z, Shum H-C. All-aqueous electrosprayed emulsion for templated fabrication of cytocompatible microcapsules. ACS Appl Mater Interfaces 2015;7(25):13925–13933.
28. Altobelli R, Guarino V, Ambrosio L. Micro-and nanocarriers by electrofludodynamic technologies for cell and molecular therapies. Process Biochem 2016;51:2143–2154.
29. Dimida S, Demitri C, De Benedictis VM, Scalera F, Gervaso F, Sannino A. Genipin-cross-linked chitosan-based hydrogels: Reaction kinetics and structure-related characteristics. J Appl Pol Sci, 2015;132:42256.

30. Cannazza G, Cataldo A, De Benedetto E, Demitri C, Madaghiele M, Sannino A. Experimental assessment of the use of a novel superabsorbent polymer (SAP) for the optimization of water consumption in agricultural irrigation process. Water 2014;6:2056–2069.

31. Shohin IE, Kulinich JI, Ramenskaya GV, Abrahamsson B, Kopp S, Langguth P, Polli JE,Shah VP, Groot DW, Barends DM, Dressman JB. Biowaiver monographs for immediate-release solid oral dosage forms: Ketoprofen. J Pharma Sci 2012;101:3593–3603.

32. Mayol L, Borzacchiello A, Guarino V, Serri C, Biondi M, Ambrosio L. Design of electrosprayed poly (L-lactide-co-glycolide) non spherical microdevices for sustained drug release. J Mat Sci: Mat Med 2014;25(2):383–390.

33. Khodir WA, Guarino V, Alvarez-Perez M, Cafiero C, Ambrosio L. Trapping tetracycline-loaded nanoparticles into polycaprolactone fiber networks for periodontal regeneration therapy. J Bioact Compat Polym 2013;28:258–273.

34. Guarino V, Altobelli R, Ambrosio L. Chitosan microgels and nanoparticles via electrofluidodynamic techniques for biomedical applications. Gels 2016;2(1):2.

35. Bevins CL, Salzman NH. Paneth cells, antimicrobial peptides and maintenance of intestinal homeostasis. Nat Rev Microbiol 2011;9: 356–368.

36. Stokke BT, Varum KM, Holme HK, Hjerde RJN, Smidsrod O. Sequence specificities for lysozyme depolymerization of partially N-acetylated chitosans. Can J Chem 1995;73(11):1972–1981.